



---

## **ELUCIDATING CHARACTERISTICS OF GEOPOLYMER WITH SOLAR PANEL WASTE GLASS**

**HuiCong Hao<sup>1</sup>, Kae-Long Lin<sup>2\*</sup>, DeYing Wang<sup>1</sup>, Sao-Jeng Chao<sup>3</sup>, Hau-Shing Shiu<sup>2</sup>,  
Ta-Wui Cheng<sup>4</sup>, Chao-Lung Hwang<sup>5</sup>**

<sup>1</sup>*Department of Environmental and Material Engineering, Yan-Tai University, China*

<sup>2</sup>*Department of Environmental Engineering, National Ilan University, Ilan 26047, Taiwan*

<sup>3</sup>*Department of Civil Engineering, National Ilan University, Ilan 26047, Taiwan*

<sup>4</sup>*Department of Materials and Mineral Resources Engineering, National Taipei University of Technology, Taiwan*

<sup>5</sup>*Department of Construction Engineering, National Taiwan University of Science and Technology, Taiwan*

---

### **Abstract**

This study examined the characteristics of geopolymers with solar panel waste glass. After 28 days of curing, the compressive strengths of the geopolymers containing 10 mass % and 20 mass % solar panel waste glass were  $63.3 \pm 1.8$  and  $49.1 \pm 2.2$  MPa, respectively. The geopolymer sample with 10% solar panel waste glass exhibited a stronger reaction than that with 20% solar panel waste glass, and the strength decreased as the amount of solar panel waste glass increased. Thermo-gravimetric and differential thermal analysis (TG/DTA) results showed that the mass loss of geopolymers after heating declined as the amount of solar panel waste glass increased. The principal peaks in the Fourier transformation infrared spectroscopy (FTIR) spectra corresponded to the Si-O-Al bond in geopolymers. Scanning electron microscopy (SEM) observations indicated that the microstructures of the stronger samples were more homogeneous, and the microstructures of geopolymers with 10% solar panel waste glass did not exhibit substantial deterioration. The experimental results indicate that solar panel waste glass has the potential to serve as a partial replacement of metakaolinite and exhibits favorable mechanical characteristics.

**Key words:** alkali-activated, compressive strength, geopolymer, metakaolinite, solar panel waste glass

*Received: February, 2012; Revised final: July, 2012; Accepted: August, 2012*

---

### **1. Introduction**

Geopolymer is a new class of building materials that is widely used worldwide in recent years. It is a type of three-dimensional aluminosilicate binder, which was developed by Davidovits (1991). It is the product of the reaction of solid aluminosilicate with a highly concentrated aqueous alkali hydroxide or silicate solution. In a strongly alkaline solution, aluminosilicate is rapidly dissolved to form free  $\text{SiO}_4$  and  $\text{AlO}_4$  tetrahedral units. As the reaction proceeds,  $\text{SiO}_4$  and  $\text{AlO}_4$  tetrahedral units are linked by oxygen atoms to yield polymeric Si-O-Al bonds, the empirical chemical formula of which is shown in (Eq. 1), where M is an alkali metal cation, such as

potassium and sodium, and n represents the degree of polycondensation; z is 1, 2, 3 (Khale and Chaudhary, 2007).



Geopolymer is an aluminosilicate material with several properties, including effective acid and fire resistance, compressive strength, durability, and an ability to immobilize toxic and radioactive materials (Duxson et al., 2007a; Komnitsas and Zaharaki, 2007; Palomo et al., 1999; Temuujin et al., 2009). Interest in geopolymers has increased in recent years because of its wide range of potential applications in civil engineering and several other

---

\* Author to whom all correspondence should be addressed: e-mail: klin@niu.edu.tw; Phone: (886) 3-9357400 ext. 7579; Fax: (886) 3-9364277

industrial sectors (Andini et al., 2008; Rovnanik, 2010; Temuujin et al., 2009).

In recent decades, the reuse and recycling of industrial solid wastes and municipal solid wastes have attracted substantial interest in Taiwan (Chiang et al., 2010; Chow et al., 2008; Ghosh and Ghosh, 2013; Lin et al., 2009, 2011; Popovici et al., 2013). According to Taiwan's Environmental Production Administration (EPA), 0.75 million tons of garbage was disposed in 2006, 5.84% of which was waste glass (Lin, 2007). The cumulative amount of waste glass that was dumped into landfills in Taiwan is approximately 0.52 million tons, whereas the amount of solar panel waste glass has reached 1000 tons. A solar panel includes crystalline silicon and a thin film. The most established thin film solar panel technology is based on amorphous silica (a-Si).

The demand for solar panels will increase the amount of produced solar panel waste glass. The conventional treatment of solar panel waste glass involves the landfill process; however, landfilling is not a favorable option because it imposes a considerable financial burden on foundries (Liao, 2009) and makes them liable for future environmental costs and problems, as required by the landfill regulations.

Solar panel waste glass comprises mainly  $\text{SiO}_2$  and can be used to prepare geopolymers. This study examined the characteristics of geopolymers that contain solar panel waste glass. The results of this study will contribute to the promotion of solar panel waste glass recycling technologies to help to achieve the goal of sustainable development and establish a recycling society with zero discharge.

## 2. Materials and methods

### 2.1. Materials

The geopolymer was synthesized from metakaolinite, which was prepared by calcining kaolinite from Pei-Long Enterprise CO., LTD. in Taiwan at  $650^\circ\text{C}$  for 3 h. Solar panel waste glass was collected from a solar panel manufacturing plant in Taiwan. The main constituents of raw materials were showed in previous study (Gao et al., 2014). The solar panel waste glass was ground to a Blaine fineness value of approximately  $360 \text{ m}^2 \text{ kg}^{-1}$ . The resultant pulverized solar panel waste glass was desiccated before being tested.

### 2.2. Experimental procedure

$\text{NaOH}$  and sodium silicate solution were mixed using an electrical mixer for five minutes and cooled to room temperature. Then, the activator was added to the metakaolinite and the powdered solar panel waste glass, and stirred for another ten minutes. The homogenous slurry was then poured into cubic plastic moulds with a volume of  $50 \text{ mm} \times 50 \text{ mm} \times 50 \text{ mm}$ .

Samples were cured in a laboratory oven at  $30^\circ\text{C}$  and an ambient pressure for 24 h before they were removed from the moulds. Experiments were carried out on the mechanical strength of the samples after the specified number of days of curing.

### 2.3. Blend ratios of the geopolymer paste samples

Table 1 presents the blend ratios of the geopolymer paste samples. The effects of solid/liquid (S/L, powder of metakaolin and solar panel waste glass to alkali solution ratio),  $\text{SiO}_2/\text{Na}_2\text{O}$  (Ms, the alkali solution contained molar of  $\text{SiO}_2$  to  $\text{Na}_2\text{O}$  ratio) on the strength of the geopolymer pastes were examined. Based on the results of the two experiments, the effects of the ratios S/L and Ms on geopolymer with solar panel waste glass were examined.

**Table 1.** The blend ratios of the geopolymer paste samples

<i>Series</i>	<i>Blend ratios of samples</i>		<i>Samples proportion by weight percent (wt %)</i>		
	S/L*	Ms**	Kaolinite	$\text{Na}_2\text{SiO}_3$	$\text{NaOH}$ (10 M)
S/C	1.0	1.0	50	26.1	23.9
	0.8	1.0	44.4	29.0	26.6
	0.6	1.0	37.5	32.6	29.9
	0.4	1.0	28.6	37.3	34.1
S/N	0.8	0.75	44.4	23.7	31.9
	0.8	1.00	44.4	29.0	26.6
	0.8	1.25	44.4	33.6	22.0
	0.8	1.50	44.4	37.5	18.1
	0.8	1.75	44.4	40.9	14.7

### 2.4. Analytical methods

The following major analyses of the geopolymers with and without solar panel waste glass were performed.

(1) Compressive strength tests were performed after 1, 7, 14 and 28 days using a  $50 \text{ mm} \times 50 \text{ mm} \times 50 \text{ mm}$  cubic sample, according to ASTM C109.

(2) Chemical composition: The samples were tested by an automated RIX 2000 spectrometer.

(3) Mineralogy: The samples were characterized by X-ray diffraction (XRD) using the  $\text{CuK}\alpha$  radiation on a Siemens D-5000 X-ray diffractometer 20 scanning, ranging between  $10^\circ$  and  $80^\circ$  and the XRD scans were run at  $0.05^\circ$ -increments, with a 1 sec counting time.

(4) Fourier transformation infrared spectroscopy (FTIR) was carried out on samples using a Bomem DA8.3 spectrometer.

(5) Scanning electron microscopy (SEM): the microstructure of the geopolymer was observed using a Hitachi S-3500N.

(6) Differential Thermal and Thermo-gravimetric Analysis (DTA/TGA): DTA/TGA analysis was done on a Seiko SSC Model 5000 Thermal Analyzer at  $25^\circ\text{C} / \text{min}$  heating rate in the  $25^\circ\text{C}-1000^\circ\text{C}$  temperature range.

### 3. Results and discussion

#### 3.1. Characteristics of raw materials

The main components of solar panel waste glass were amorphous, as revealed by their broad diffuse bands. The main crystalline component identified in kaolinite is quartz and  $(\text{Al}_2[\text{Si}_2\text{O}_5](\text{OH})_4)$ . During the transition from kaolinite to metakaolinite, the kaolinite structure disappeared and was amorphous. XRD patterns of raw materials are presented in the work of Hao et al. (2013).

Fig. 1 presents the FTIR spectra of the raw materials. The peaks of waste glass around  $470 \text{ cm}^{-1}$ ,  $1008 \text{ cm}^{-1}$ ,  $1031 \text{ cm}^{-1}$  and  $1087 \text{ cm}^{-1}$  correspond to the asymmetric stretching of Si-O-Si. Kaolinite presented the asymmetric stretching of Si-O-Si around  $470 \text{ cm}^{-1}$ ,  $540 \text{ cm}^{-1}$ ,  $880 \text{ cm}^{-1}$  and  $950\text{-}1200 \text{ cm}^{-1}$ , which were attributed to Si-O-Si bending, the octahedral of Si-O-Al, asymmetric stretching of Si-O-Si and the asymmetric stretching of T-O-Si (T: Si or Al), respectively. The bands around  $917 \text{ cm}^{-1}$  was related to the OH bending. The peaks around  $3640 \text{ cm}^{-1}$  and  $1680 \text{ cm}^{-1}$  correspond to the bending vibration of HOH. The peaks of metakaolinite around  $950\text{-}1200 \text{ cm}^{-1}$  related to T-O-Si.

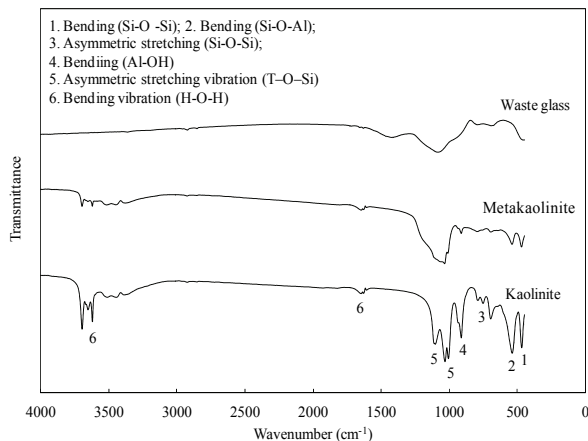


**Fig. 1.** FTIR spectra of raw materials

#### 3.2. Compressive strength of geopolymer without solar panel waste glass

Fig. 2 shows the compressive strength of the S/C series from Table 1 as a function of S/L (S/L: powder of metakaolin and solar panel waste glass to alkali solution ratio). The compressive strength increased in conjunction with S/L for a specific curing time. The compressive strength of the geopolymer increased as curing time (except for S/L = 0.6 and S/L = 0.4 at 28 days). The strength increased rapidly after the first 24 hours, and subsequently increased slowly. The relationship between silica and alumina in the metakaolin-based geopolymer system is responsible for the increase in strength (Somna et al., 2011). The compressive strength of geopolymer at an S/L of 0.6 or 0.4 decreased after 14 days, because the geopolymer

contained excess water at a low S/L. At 1-day and 28-days, the strength of the geopolymer with an S/L of 0.8 was 42.12 and 48.34 MPa, respectively (slightly lower than for the geopolymer with an S/L of 1.0); when the S/L was 1.0, the mixtures were sticky and difficult to pour into the mold. Therefore, from a practical point of view, the optimal S/L was 0.8.

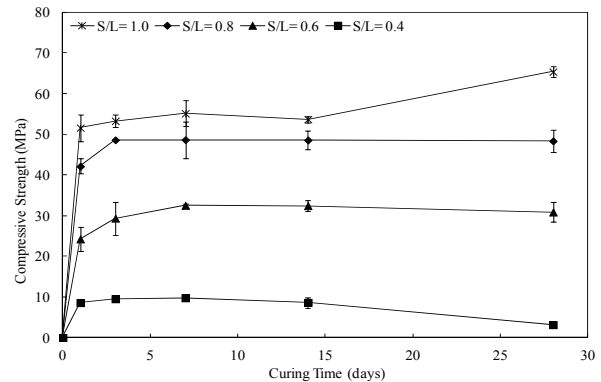


**Fig. 2.** Compressive strength of geopolymer without glass for various S/L

Fig. 3 shows the results of the compressive strength tests on the S/N series, and Table 1 shows various Ms ratios.

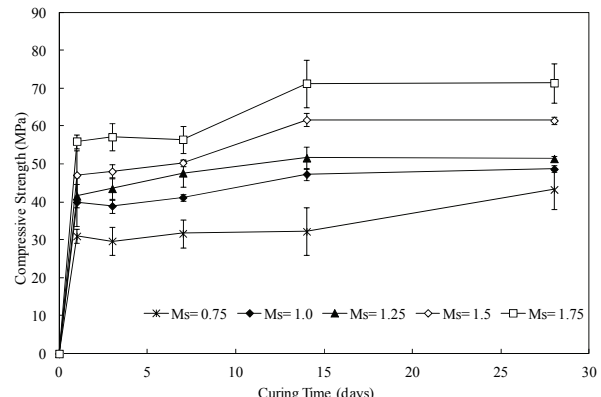


**Fig. 3.** Compressive strength of geopolymer without glass for various Ms

The effect of Ms on the strength was similar to that of S/C series, and increased in conjunction with curing time. The compressive strength of the geopolymer increased in conjunction with Ms. The increase in the strength of the geopolymer in conjunction with the silica content may have occurred because Si-O-Si bonds are stronger than Si-O-Al bonds (Duxson et al., 2005). The graph shows that the strength of geopolymer with an Ms of 1.75 was 56.02 MPa at 1-day and 71.42 MPa at 28-days. The results indicate that geopolymer with a higher Ms had a higher compressive strength. Therefore, the optimal Ms was 1.75.

#### 3.3. Compressive strength of geopolymers with and without solar panel waste glass

Fig. 4 shows the compressive strength of the geopolymer with solar panel waste glass for S/L 0.8

and Ms 1.75. The compressive strength increased in conjunction with curing time, and decreased as the solar panel waste glass content increased. At 28 days of curing, the compressive strength of the geopolymer with 10% solar panel waste glass was 63.27 MPa, which was 88.2% that of pure metakaolinite geopolymer, and the compressive strength of the geopolymer with 20% solar panel waste glass was 49.06 MPa.

The compressive strength decreased as the amount of solar panel waste glass increased, because the excess solar panel waste glass, which supplied the silica, reduced the aluminum that was in metakaolinite; therefore, it was more difficult to synthesize the aluminosilicate. Therefore, the optimal amount of waste glass in the geopolymer was 10%, which demonstrated the use of waste glass in the geopolymer mixture by partial substitution of costly metakaolinite with the cheaper waste glass without considerable deterioration of the geopolymer.

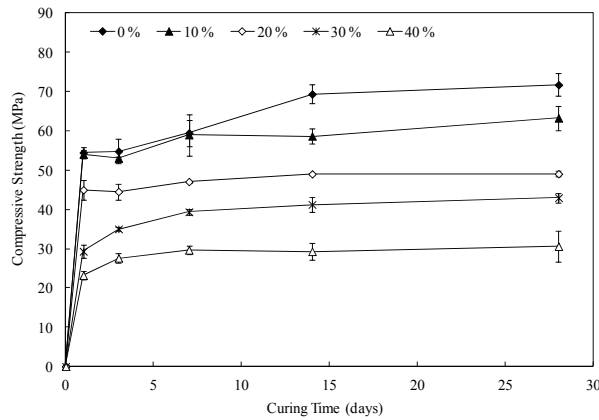


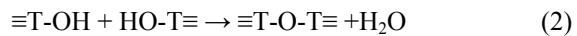
**Fig. 4.** Compressive strength of geopolymer with solar panel waste glass

### 3.4. Differential thermal and thermogravimetric analyses of geopolymers with and without solar panel waste glass

Water is a crucial structural component of a geopolymer. The loss of mass of a geopolymer may be attributed to the evaporation of absorbed and bonded water. The absorbed water is lost at temperatures less than 100°C; increase of temperature results in shrinkage and damages the geopolymer structure (Daniel et al., 2008). The remaining water is either bound tightly or is less able to diffuse to the surface and continues to evaporate slowly at higher temperatures (Riessen, 2007). The continuous weight loss up to almost 500 °C is caused by the evaporation of hygroscopic water or water residing in the channels (Perraki et al., 2005).

TG/DTA was used to determine the mass loss of the geopolymer with solar panel waste glass for S/L 0.8 and Ms 1.75. Fig. 5 shows the DTA curves of geopolymer with solar panel waste glass after 28 days of curing. An endothermic peak of the DTA curve was observed at approximately 100- 400°C, revealing an obvious mass loss. This peak was mainly associated with the evaporation of free pore

water (Duxson et al., 2006). The second endothermic peak appeared from 480 to 600°C; the endothermic peak can be caused by the elimination of water by condensation of silanol or aluminol groups on the surface of the geopolymeric gel. Eq. 2 shows the exothermic reaction, where T is either Al or Si (Duxson et al., 2007b). No apparent mass loss of metakaolinite geopolymer was observed from 650 to 770°C.



The TG of the geopolymer with solar panel waste glass followed a similar trend to that of pure metakaolinite geopolymer. When the amount of waste glass reached 40%, the endothermic peaks at approximately 600°C and 770°C, associated with the condensation of silanol and aluminol groups of the gel, were more obvious than those of other geopolymers, because the geopolymer with 40% waste glass comprised gel and unreacted waste glass, which does not yield an endothermic peak at the relevant temperature. Therefore, the endothermic peak is more obvious than that obtained from any other geopolymer, the signals from which may be disturbed by the unreacted metakaolinite. Geopolymers with 30 and 40% of waste glass, the third endothermic peak appeared from 650 to 770°C. It was the nucleation temperature of waste glass (Tulyaganov et al., 2002), because the geopolymer with 30 and 40% waste glass comprised unreacted waste glass.

Fig. 6 shows the loss of mass of geopolymer at various temperatures. The loss of mass of the geopolymer with solar panel waste glass at approximately 100- 400°C and 480- 600°C exceeded that at 650- 770°C. The results are consistent with several studies, which observed lower loss of mass at higher temperatures (Duxson et al., 2006).

At 28 days, the mass losses at 100-400°C of the pure metakaolinite geopolymer and the geopolymers with 10% and 40% waste glass were 17.75%, 19.75%, 19.36%, respectively. After heating to 480-600°C and 650-770°C, the mass loss of the geopolymer with 40% waste glass was 6.09% and 1.67%. At a specific curing time, the mass loss by the evaporation of free pore water and condensation of silanol or aluminol groups in the gel for the geopolymer indicated that the mass loss can be reduced by increasing the amount of waste glass. This observation is consistent with the development of compressive strength.

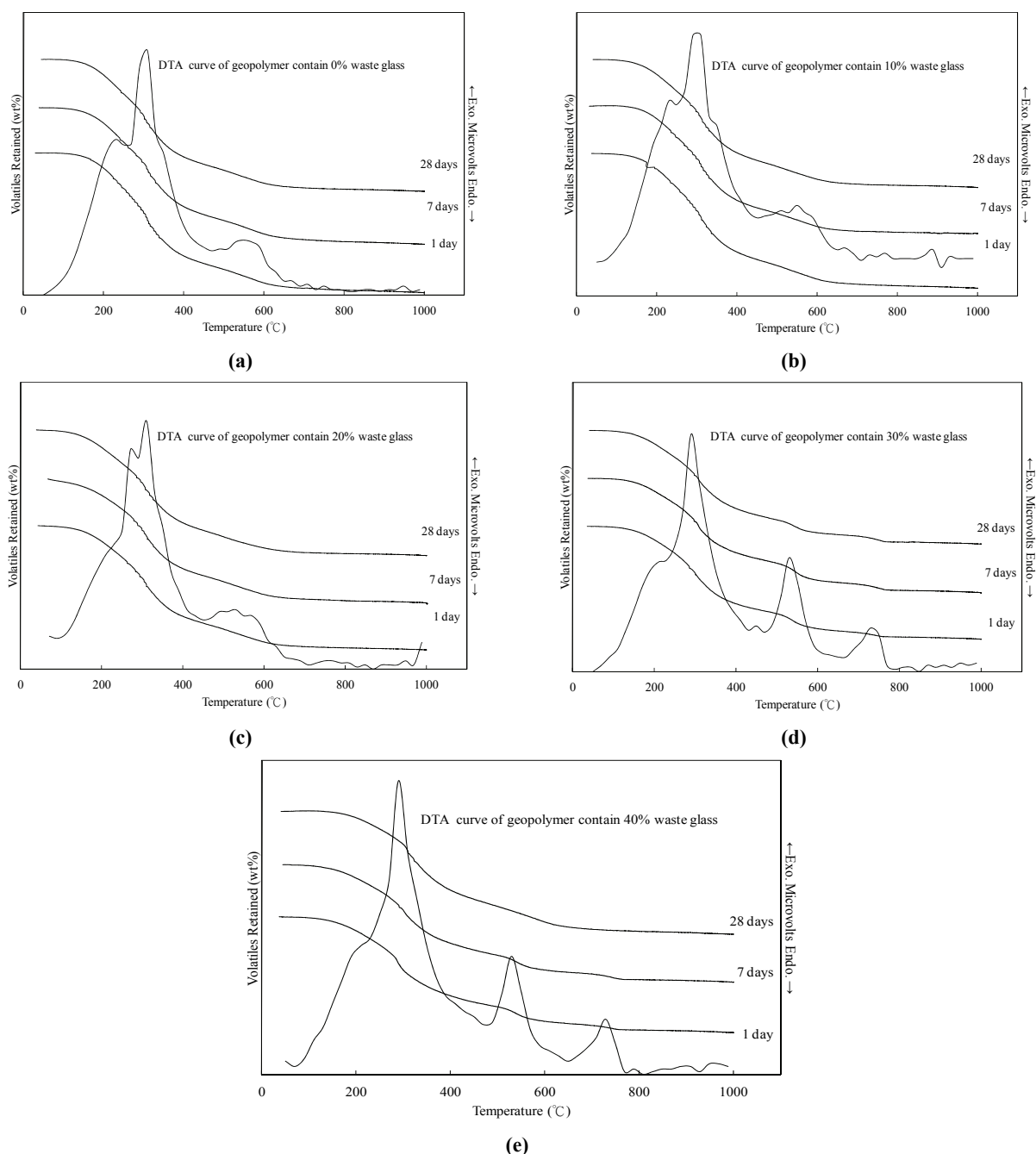
### 3.5. FTIR spectra of geopolymers with and without solar panel waste glass

Fig. 7 shows the FTIR spectra of the geopolymers that contained solar panel waste glass for S/L 0.8 and Ms 1.75. Table 2 shows the absorption peak of the geopolymer after curing for 28 days. Table 2 shows the peaks around 3420  $\text{cm}^{-1}$  and 1680  $\text{cm}^{-1}$  in the FTIR spectrum of the geopolymer

are associated with the adsorbed water that remained in the geopolymer sample after polycondensation. Fig. 7 shows the peaks around 1033 and 1009 cm<sup>-1</sup> correspond to the individual tetrahedra asymmetric stretching of Al–O and Si–O bonds. However there is a slight shifting of 1008 cm<sup>-1</sup> peak towards higher wave-numbers which might be the result of the formation of a structure at which the SiO<sub>4</sub><sup>4-</sup> groups are replaced by AlO<sub>4</sub><sup>3-</sup> groups as network formers. These bonds exhibited higher wavenumbers than raw materials, which indicated that the bonding structures changed in individual tetrahedral (Van Jaarsveld et al., 2002). The peaks around 810 and 539 cm<sup>-1</sup> were associated with the Si–O–Al vibration of the

geopolymer, indicating that the principal peaks were associated with the Si–O–Al bond in the geopolymer following geopolymerization (Barbosa et al., 2000; Van Jaarsveld et al., 2002).

During alkali activation of metakaolinite, major disruption of the Al environment is indicated by the loss of the Si–O–Al band at 810 cm<sup>-1</sup> which is replaced by several weaker bands in the range 600–800 cm<sup>-1</sup> (Barbosa et al., 2000). The study results (Table 2) confirm the loss of the Si–O–Al band at 811 cm<sup>-1</sup>. The band at 467 cm<sup>-1</sup> is attributed to Si–O flexural vibration (Wang et al., 2005). The band around 917 cm<sup>-1</sup> was related to the Al–O–Si bond.



**Fig. 5.** TG/DTA curves of geopolymers with and without solar panel waste glass(a) 0%, (b) 10%, (c) 20%, (d)30%, (e) 40%

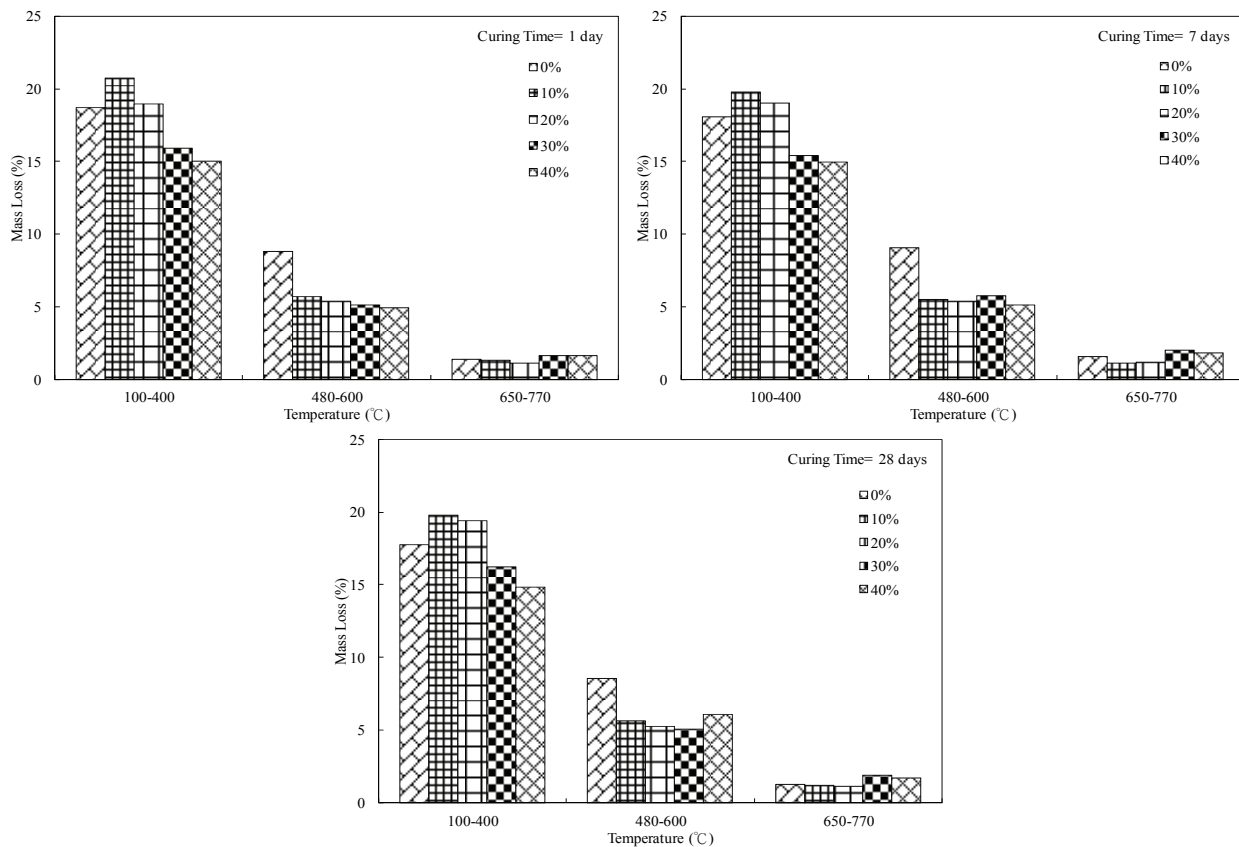


**Fig. 6.** Mass loss of geopolymers with and without solar panel waste glass

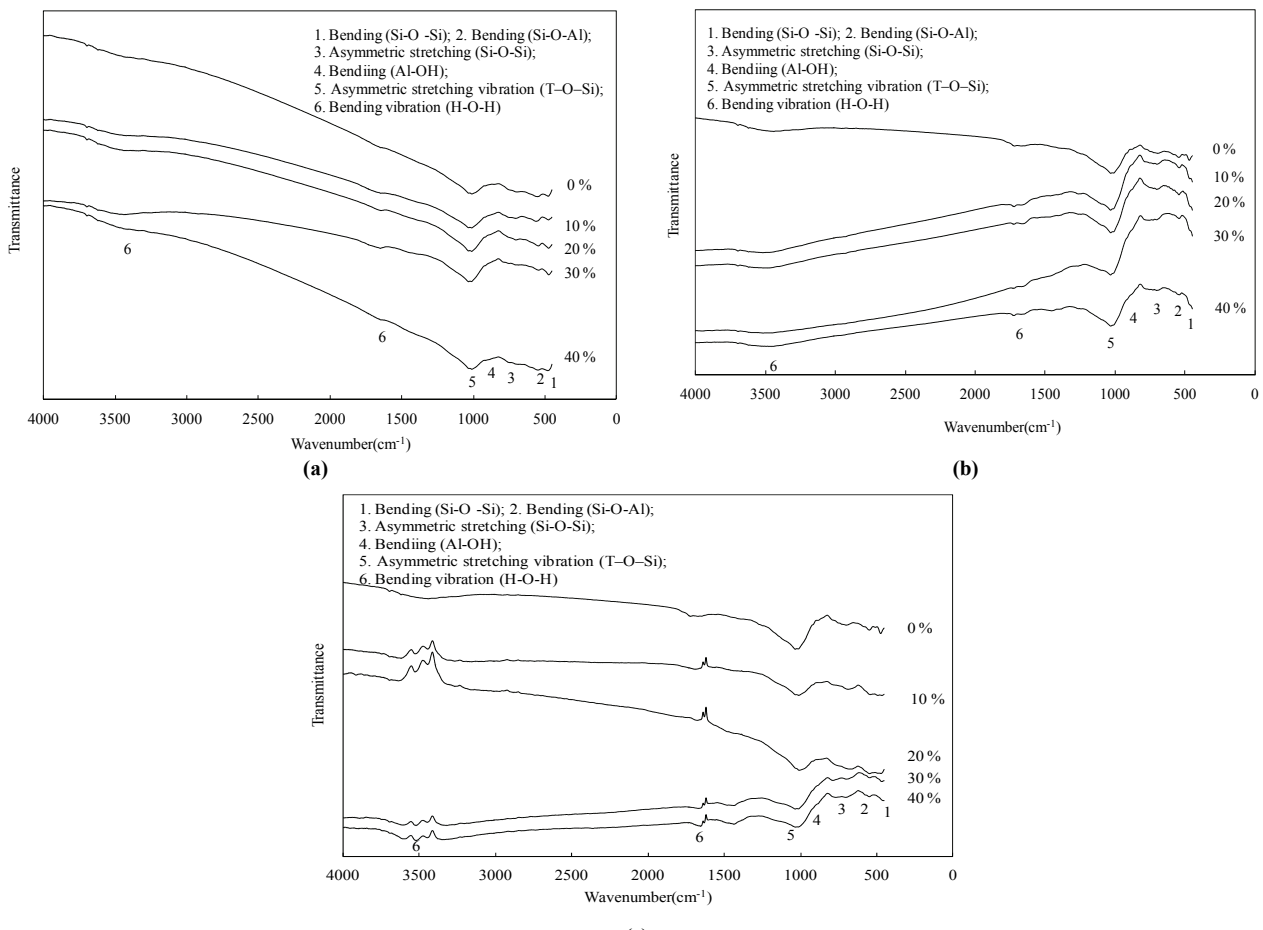


**Fig. 7.** FTIR patterns of geopolymers with and without solar panel waste glass. (a) 1 day, (b) 7 days, (c) 28 days

**Table 2.** FTIR absorption peaks for geopolymer at 28 days of curing

Matrix	Wavenumber ( $\text{cm}^{-1}$ )						
Waste glass	470	540	-		1008	1031	1087
Metakaolinite	474	540	811	-	-	1036	1068
Kaolinite	470	540	-	915	1008	1031	
0%	470	547	-	-	1012	1036	
10%	464	540	-	-	1010	1029	
20%	468	543	-	-	1006	-	
30%	-	543	-	-	1012	1033	
40%	-	545	-	-	1012	1031	

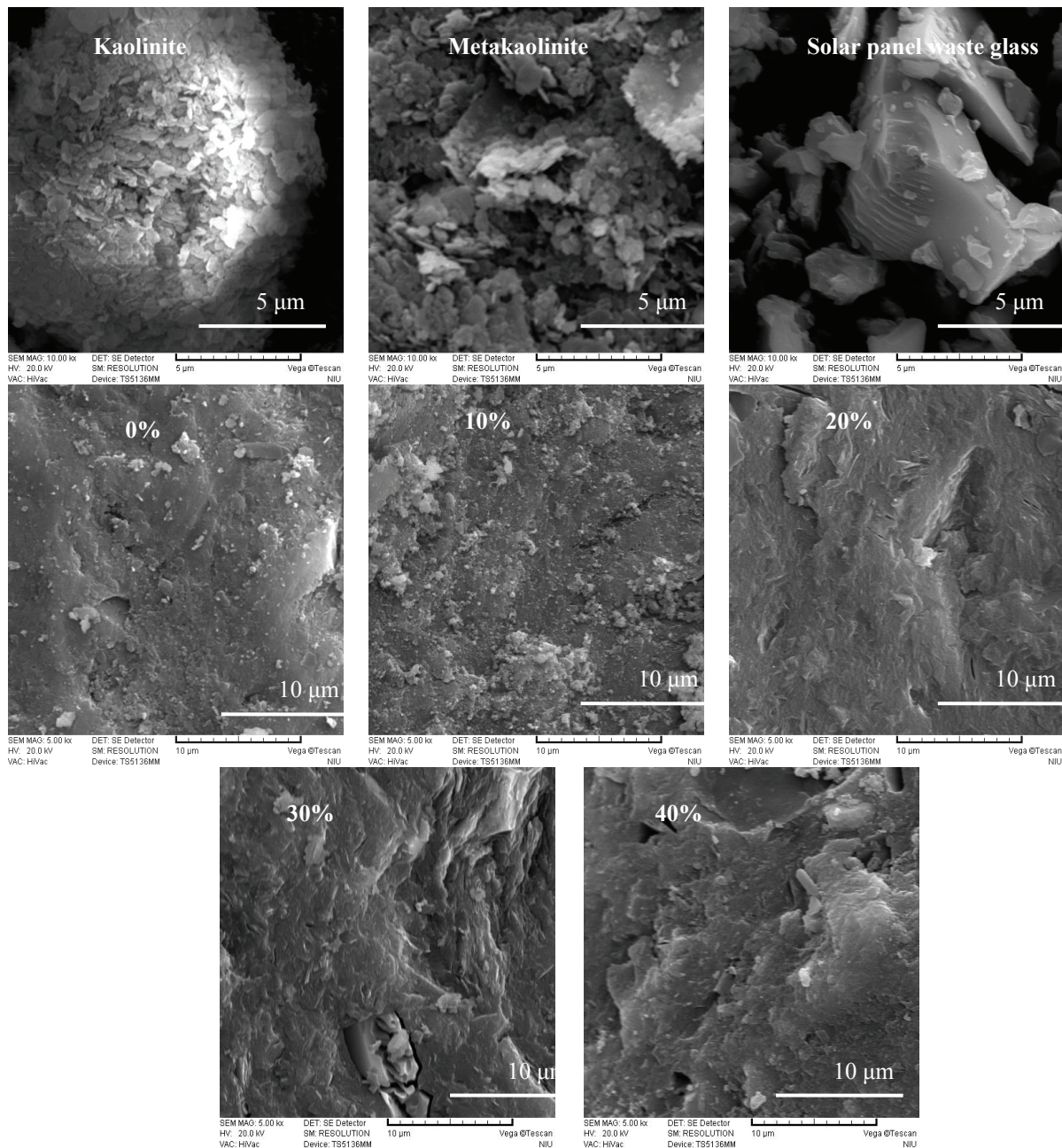


**Fig. 8.** SEM micrographs of raw materials and geopolymers with and without panel waste glass

### 3.6. SEM observation of geopolymers with and without solar panel waste glass

Fig. 8 shows the SEM micrographs of the raw materials and geopolymers with and without solar

panel waste glass that was aged for 28 days with S/L 0.8 and Ms 1.75. Kaolinite has a typical layered structure, such as metakaolinite. The micrograph of the raw materials indicated that the size of the particles in the solar panel glass exceeded those in

kaolinite and metakaolinite, the microstructures of which included an obvious interface and large pores. A previous study indicated that the main components of geopolymers are unreacted aluminosilicate particles and the gel phase (Kumar and Kumar, 2011; Lloyd et al., 2009). The observed gel with an amorphous structure is present in the geopolymer system and adheres to the product and unreacted particles. A geopolymer with more gel is denser, has a more homogenous microstructure and higher mechanical strength (Matthew and Brian, 2003).

The structure of the geopolymers with 10% waste glass was similar to that of the pure metakaolinite geopolymer, which was dense and homogenous. The SEM micrographs of the geopolymer with 30% and 40% waste glass differed considerably.

The main microstructure of geopolymer with 30% and 40% waste glass was inhomogeneous and non-compact, with unreacted material and several pores. These results suggest that the microstructures of stronger samples were more homogeneous and the microstructures of weak samples were highly inhomogeneous and incompact.

#### 4. Conclusions

This study demonstrated the use of solar panel waste glass as a partial substitute for metakaolinite in the production of geopolymers. At 28 days of curing, the compressive strengths of geopolymers with 10% and 20% waste glass were 63 and 50 MPa, respectively. FTIR spectra indicated that the principal peaks were attributable to Si-O-Al bonds in the geopolymer. These results indicated that the optimal amount of waste glass in the geopolymer was 10%, which demonstrated the use of waste glass in the geopolymers by partial substitution of costly metakaolinite with the cheaper waste glass without considerable deterioration of geopolymer.

#### Acknowledgement

The authors would like to thank the National Science Council of the Republic of China, Taiwan, for financially supporting this research under Contract No. NSC 99-2622-E-197-003-CC 3 and NSC 101-2923-I-011-001-MY4.

#### References

- Andini S., Cioffi R., Colangelo F., Grieco T., Montagnaro F., Santoro L., (2008), Coal fly ash as raw material for the manufacture of geopolymer-based products, *Waste Management*, **28**, 416–423.
- Barbosa V.F.F., MacKenzie K.J.D., Thaumaturgo C., (2000), Synthesis and characterisation of materials based on inorganic polymers of alumina and silica: sodium polysialate polymers, *International Journal of Inorganic Materials*, **2**, 309–317.
- Chiang K.Y., Chen Y.C., Chien K.L., (2010), Scrap glass effect on building materials characteristics manufactured from water treatment plant sludge, *Environmental Engineering Science*, **27**, 137-145.
- Chow J.D., Chai W.L., Yeh C.M., Chuang F.S., (2008), Recycling and application characteristics of fly ash from municipal solid waste incinerator blended with polyurethane foam, *Environmental Engineering Science*, **25**, 461-474.
- Davidovits J., (1991), Geopolymers: Inorganic polymer new materials, *Journal of Thermal Analysis and Calorimetry*, **37**, 1633-1656.
- Duxson P., Provis J.L., Lukey G.C., Mallicoat S.W., Kriven W.M., van Deventer J.S.J., (2005), Understanding the relationship between geopolymer composition, microstructure and mechanical properties, *Colloids and Surfaces A: Physicochemical and Engineering Aspects*, **269**, 47–58.
- Duxson P., Lukey G.C., van Deventer J.S.J., (2006), Thermal evolution of metakaolin geopolymers: Part 1-Physical evolution, *Journal of Non-Crystalline Solids*, **352**, 5541–5555.
- Duxson P., Lukey G.C., Van Deventer J.S.J., (2007a), Physical evolution of Na-geopolymer derived from metakaolin up to 1000°C, *Journal of Materials Science*, **42**, 3044 – 3054.
- Duxson P., Fernandez-Jimenez A., Provis J.L., Lukey G.C., Palomo A., van Deventer J.S.J., (2007b), Geopolymer technology: the current state of the art, *Journal of Materials Science*, **42**, 2917–2933.
- Ghosh M.K., Ghosh U.K., (2013), Utilization of agroindustrial waste and dairy waste in solid state production of lactic acid, *Environmental Engineering and Management Journal*, **12**, 2501–2509.
- Hao H.C., Lin K.L., Wang D.Y., Chao S.J., Shiu H.S., Cheng T.W., Chao-Lung Hwang C.L., (2012), Recycling of Solar Panel Waste Glass as a Partial Replacement of Meta-kaolinite in the Production of Geopolymers, *The Open Civil Engineering Journal*, **6**, 239-248.
- Khale D., Chaudhary R., (2007), Mechanism of geopolymerization and factors influencing its development: a review, *Journal of Materials Science*, **42**, 729–746.
- Komnitsas K., Zaharaki D., (2007), Geopolymerisation: a review and prospects for the minerals industry. *Minerals Engineering*, **20**, 1261–1277.
- Kumar S., Kumar R., (2011), Mechanical activation of fly ash: Effect on reaction, structure and properties of resulting geopolymer, *Ceramics International*, **37**, 533–541.
- Liao Y.H., (2009), A Study on the Material Flow and Management of Solar Cell and Panel in Taiwan, Master thesis, Institute of Environmental Engineering and Management (in Chinese).
- Lin K.L., (2007), Use of thin film transistor liquid crystal display (TFT-LCD) waste glass in the production of ceramic tiles, *Journal of Hazardous Materials*, **148**, 91– 97.
- Lin K.L., Lin D.F., Chao S.J., (2009), Effects of municipal solid waste incinerator fly ash slag on the strength and porosity of slag-blended cement pastes, *Environmental Engineering Science*, **26**, 1081-1086.
- Lin K.L., Cheng C.J., Shie J.L., Chao S.J., Cheng A., Hsu H.M., Hwang C.L., (2011), Effect of using shell molding sand and sodium silicate sand as substitute sources for cement raw materials, *Environmental Engineering Science*, **28**, 653-660.
- Lloyd R.R., Provis J.L., van Deventer J.S.J., (2009), Microscopy and microanalysis of inorganic polymer cements. 2: the gel binder, *Journal of Materials Science*, **44**, 620–631.

- Matthew R., Brian C., (2003), Chemical optimisation of the compressive strength of aluminosilicate geopolymers synthesised by sodium silicate activation of metakaolinite, *Journal of Materials Chemistry*, **13**, 1161- 1165.
- Palomo A., Grutzeck M.W., Blanco M.T., (1999), Alkali-activated fly ashes: A cement for the future, *Cement and Concrete Research*, **29**, 1323–1329.
- Popovici A., Rusu T., Tofana V., Dan V., Popita G.E., Hategan R., Marutoiu C., (2013), Study on recycling feasibility of activated glass from WEEE equipment treatment, *Environmental Engineering and Management Journal*, **12**, 359-364.
- Rovanik P., (2010), Effect of curing temperature on the development of hard structure of metakaolin-based geopolymer, *Construction and Building Materials*, **24**, 1176– 1183.
- Somna K., Jaturapitakkul C., Kajitvichyanukul P., Chindaprasirt P., (2011), NaOH-activated ground fly ash geopolymer cured at ambient temperature, *Fuel*, **90**, 2118–2124.
- Temuujin J., Minjigmaa A., Rickard W., Melissa L., Williams I., van Riessen A.V., (2009), Preparation of metakaolin based geopolymer coatings on metal substrates as thermal barriers, *Applied Clay Science*, **46**, 265– 270.
- Temuujin J., Williams R.P., van Riessen A., (2009), Influence of calcium compounds on the mechanical properties of fly ash geopolymer pastes, *Journal of Hazardous Materials*, **167**, 82-88.
- Tulyaganov D.U., Ribeiro M.J., Labrinch J.A., (2002), Development of glass-ceramics by sintering and crystallization of fine powders of calcium-magnesium-aluminosilicate glass, *Ceramics International*, **28**, 515–520.
- Van Jaarsveld J.G.S., van Deventer J.S.J., Lukey G.C., (2002), The effect of composition and temperature on the properties of fly ash and kaolinite-based geopolymers, *Chemical Engineering Journal*, **89**, 63– 73.
- Wang H.L., Li H.H., Yan F.Y., (2005), Synthesis and mechanical properties of metakaolinite-based geopolymer, *Colloids and Surfaces A: Physicochemical and Engineering Aspects*, **268**, 1–6.